3 CT in Kidney Cancer

Sheila Sheth and Elliot K. Fishman

CONTENTS

S. Sheth, MD
Associate Professor of Radiology and Pathology, Johns Hopkins University School of Medicine, Director, Biopsy Service, Department of Radiology, Johns Hopkins Hospital, 600 North Wolfe Street, HAL B176D, Baltimore, MD 21287, USA
E. K. Fishman, MD, FACR
Professor of Radiology and Oncology, Johns Hopkins University School of Medicine, Director, Diagnostic Radiology and Body CT, Department of Radiology, Johns Hopkins Outpatient Center, 601 North Caroline Street, Room 3254, Baltimore, MD 21287, USA

3.1 Introduction

The past two decades have witnessed significant changes in the presentation, diagnosis, and management of renal tumors. With the widespread use of cross-sectional imaging, over one-third of renal cell carcinomas (RCC) are discovered serendipitously, and the majority of these incidental tumors are stage T1 lesions (Leslie et al. 2003). Paralleling this clinical-stage migration, there is a growing trend for more limited surgical resection, such as adrenal-sparing radical nephrectomy, laparoscopic nephrectomy, or partial, nephron-sparing, nephrectomy (Russo 2000). Computed tomography (CT) plays a central role in the evaluation of a patient with a suspected renal mass, not only in the detection but also in the characterization of the mass. Renal lesions are among the most common incidental findings on ultrasound or abdominal CT (Carrim and Murchison 2003). The vast majority are cysts that do not require any further management. If, however, the mass is not obviously a simple cyst, it becomes critical to differentiate between minimally complicated cysts, which can be observed. and potentially malignant lesions which require surgical removal. In patients with solid renal masses, CT is an essential tool for staging and surgical planning.

In this chapter we review state-of-the art CT techniques for evaluation of the kidneys. We discuss CT protocols best suited for detection of small renal tumors, emphasize important findings pertinent to characterization of renal masses, and briefly outline CT strategies for staging malignant renal tumors.

3.2 CT Techniques

3.2.1 Phases of Renal Enhancement

Single and multidetector CT (MDCT) have dramatically refined the diagnostic evaluation of renal

pathology by allowing rapid image acquisition through the entire kidney during various phases of contrast enhancement and excretion following the administration of a single bolus of intravenous iodinated contrast medium.

Four distinct phases of renal enhancement can be imaged depending on acquisition time (Fig. 3.1). The timing of these phases varies with the speed of intravenous contrast injection. We routinely inject 100–120 ml of non-ionic contrast in a large antecubital vein at a rate of 3 ml/s:

1. The arterial phase. During this short phase, which occurs at about 15–25 s after the initiation of intravenous contrast injection, there is maximum opacification of the renal arteries. The renal veins also usually opacify in the late arterial phase. This phase is important for imaging potential renal donors or patients with suspected renal arterial pathology.
2. The corticomedullary phase (also called angionephrographic or late arterial phase; CMP/AP). This phase starts at about 25–70 s after the initiation of intravenous contrast injection. There is intense enhancement of the renal cortex due to preferential arterial flow to the cortex and glomerular filtration of the contrast material, while the medulla remains relatively less enhanced. This phase provides information about the vascularity of solid renal masses and is also the best phase for maximum opacification of the renal veins.
3. The nephrographic phase (also called the parenchymal venous phase; NP/VP) begins at 80–120 s. In this phase the contrast filters through the glomeruli into the collecting ducts and provides homogeneous enhancement of the normal renal parenchyma. This is the best phase for the detection of subtle parenchymal lesions.
4. The excretory phase (EP) starts at 180 s. Excretion of the contrast material allows opacification of the calyces, renal pelves, and ureters, while the intensity of the nephrogram progressively declines. We routinely acquire excretory phase images at 240 s to ensure opacification of the ureter (Fig. 3.1).

For evaluation of renal masses, a minimum of three acquisition sequences are required for detection as well as characterization of renal lesions. An initial series of unenhanced scans through the kidneys should be part of every protocol for evaluation of a suspected renal mass: it provides a baseline to measure the enhancement within the lesion after the administration of intravenous contrast. This enhancement characteristic is very important in distinguishing hyperdense cysts from solid tumors.

Our protocol for imaging a patient with a suspected renal mass follows.

Studies are performed using a 16-row-detector CT scanner (Siemens Sensation 16 scanner, Siemens Medical Solutions, Malvern, Pa.):

1. Precontrast image acquisition through the kidneys with 16×0.75-mm detector collimation, 0.75-mm slice thickness, 12 mm per rotation table speed, 5-mm reconstruction increment.
2. Late arterial phase (AP) acquisition through the kidney obtained 25 s after the start of injection of 120 ml iohexol at an injection rate of 3 ml/s with 16×0.75-mm detector collimation, 0.75-mm slice

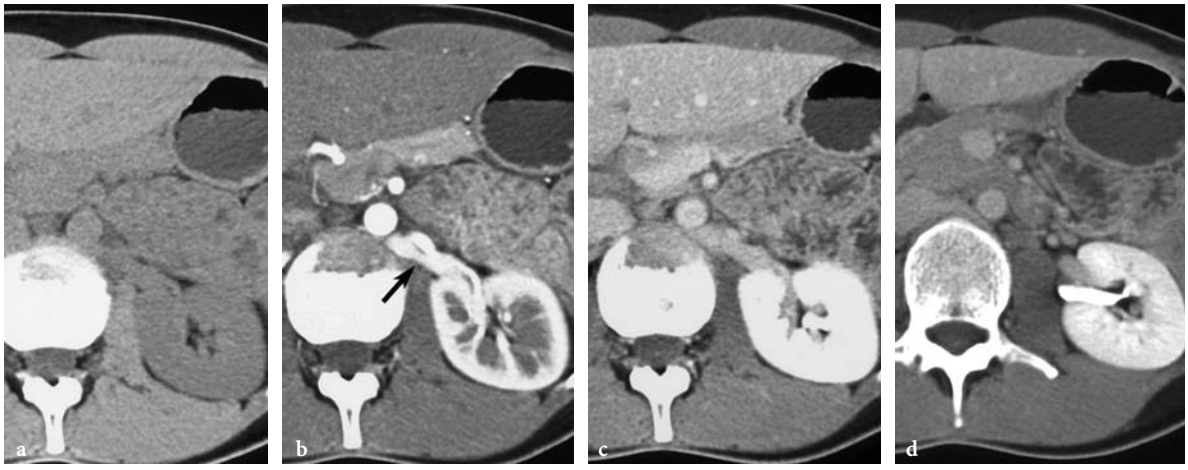

Fig. 3.1a-d. Phases of renal enhancement at CT in a 42-year-old woman with history of hematuria. **a** Axial precontrast CT scan. **b** Axial contrast-enhanced corticomedullary (late arterial phase [AP]) CT scan. Note excellent opacification of the retro-aortic left renal vein (*arrow*). **c** Axial contrast-enhanced nephrographic (parenchymal venous phase [VP]) CT scan. **d** Axial contrast-enhanced excretory phase (EP) CT scan.

thickness, 12-mm per rotation table speed, and 0.5-mm reconstruction increment. This phase depicts the renal arterial anatomy as well as the status of the renal vein, critical information for tumor staging as well as planning for surgery.
3. Delayed (excretory) phase (EP) acquisition through the abdomen and pelvis obtained after 180 to 240 s with 16×0.75-mm detector collimation, 0.75-mm slice thickness, 12 mm per rotation table speed, and 0.5-mm reconstruction increment.

We usually limit image acquisition to three sequences to minimize radiation to the patients. An additional venous phase (VP) acquisition (obtained at 55 s, with same scanning parameters as the arterial phase) can be added in select circumstances.

3.2.2 Advantages of Multidetector CT

Several advantages of multidetector CT over older-generation single-detector CT are well documented in the literature. It allows faster data acquisition times (average 2.6 times for a four-detector-row CT) when compared with single-detector CT, with no loss in image quality. Very rapid data acquisition times are possible because of short gantry rotation times (0.5 s) combined with multiple detectors providing increased coverage along the z axis (Hu et al. 2000; Foley 2003). Timing of the contrast bolus can thus be optimized to evaluate the arterial and venous supply of the kidney as well as the renal parenchyma and collecting system, and images of the entire kidneys and collecting systems can be generated during multiple phases of parenchymal enhancement and contrast excretion. Another advantage of MDCT is improved z-axis spatial resolution. The 16-detector-row scanners combine rapid data acquisition with narrow collimation. Thinner collimation greatly improves the quality of three-dimensional (3D) data sets and allows generation of excellent 3D images of the renal arteries and veins and the collecting system, comparable to those of conventional angiography and urography.

3.2.3 Post-Processing Techniques

Efficient interactive workstations are essential to handle the high number of images generated with MDCT and to generate reconstructed images simulating conventional angiographic or urographic images. Maximum intensity projection (MIP), multiplanar reconstruction, and volume-rendering (VR) techniques have been shown to be very effective. Volume rendering uses attenuation information from the entire data set by assigning shades of gray to varying attenuation values. It allows the viewer to interact with the data sets in real time, obviating the need for complex editing (Rubin 2001). It is invaluable in planning surgical management. Urologists find the interactive display of a 3D model of the affected kidney and its vascular supply particularly helpful before considering partial (nephron-sparing) nephrectomy, undertaking venous thrombectomy, and for planning extensive resection to remove a locally invasive renal cell or transitional cell cancer.

3.3 Detection and Characterization of Renal Masses

3.3.1 Detection of Renal Masses

Unlike the renal parenchyma, renal masses do not contain functioning renal nephrons. After the patient receives intravenous iodinated contrast, renal lesions exhibit varying degree of enhancement depending on their vascularity. Vascular tumors display maximum enhancement in the AP; however, in the delayed phases (VP and EP), almost all renal masses have lower attenuation than the homogeneously enhancing surrounding normal renal tissue. Many studies have demonstrated that the VP is more sensitive than the AP for the detection of small (<3 cm) renal lesions (Fig. 3.2; Cohan et al. 1995; Kopka et al. 1997; Szolar et al. 1997; Yuh and Cohan 1999). In one study that examined 295 lesions smaller than 3 cm, 84 more renal masses were seen in the VP than in the AP. This increased conspicuity was due to a statistically significant higher difference in attenuation values between the small lesions and the renal parenchyma in the VP, compared with the AP (Szolar et al. 1997). The difference was most striking for the smallest lesions (<1.1 cm) and those located in the medullary portion of the kidney (Cohan et al. 1995; Szolar et al. 1997). The AP was associated with a higher number of false-negative results as well as false-positive results. A small hypervascular solid tumor

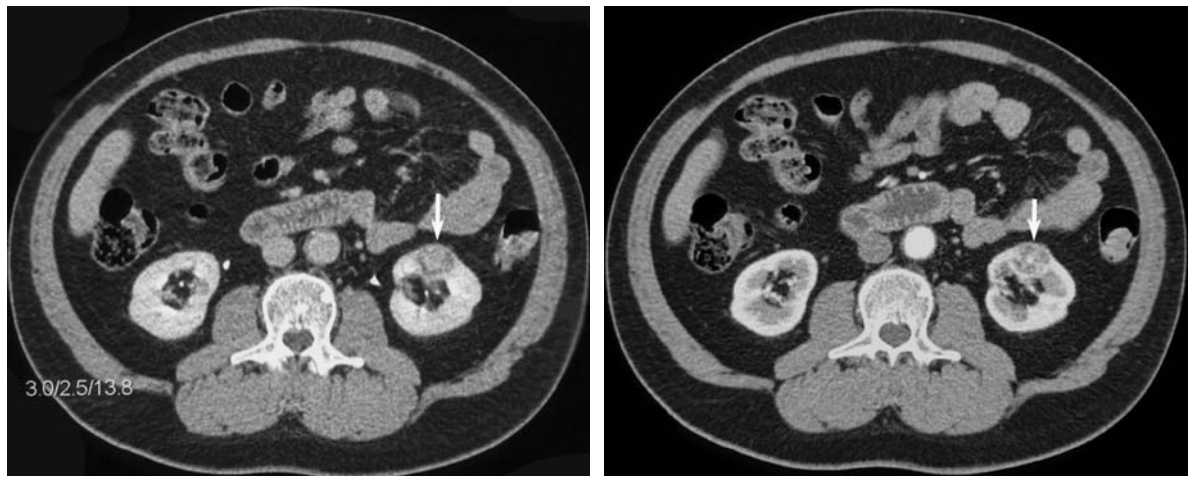

Fig. 3.2a,b. Incidental renal mass in a 58-year-old man. **a** Axial contrast-enhanced CT scan in the EP shows a 2.5-cm mass in the left kidney (*arrow*). **b** Axial contrast-enhanced CT scan in the AP shows the mass is subtle and could be mistaken for an unenhanced medulla (*arrow*). The patient underwent nephron-sparing surgery for a conventional renal cell carcinoma.

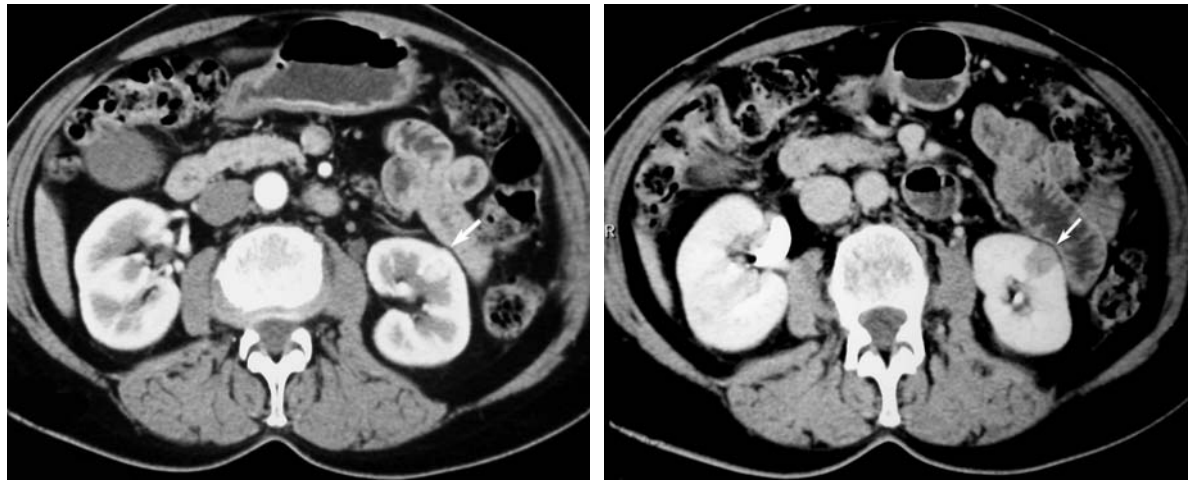

Fig. 3.3a,b. Incidental renal mass in a 64-year-old woman. **a** Axial contrast-enhanced CT scan in the AP shows a small hypervascular mass (*arrow*) in the mid portion of the left kidney which is barely visible. **b** Axial contrast-enhanced CT scan in the EP clearly shows a 2-cm mass (*arrow*) which is hypodense to the renal parenchyma in this phase. Partial left nephrectomy was performed and pathology revealed a small angiomyolipoma.

may enhance to the same degree as the renal cortex and may be mistaken for normal parenchyma on the AP (Fig. 3.3). A more common source of error (false negative) occurs when a centrally located mass is mistaken for the normal hypoenhancing medulla. On the other hand, mistaking a heterogeneously enhancing medulla for a solid tumor is a potential cause of a false-positive diagnosis.

Many of the additional small lesions detected on the VP have been shown to be clinically insignificant renal cysts (Fig. 3.4) or are too small to characterize (Cohan et al. 1995), although it appears that a significant number of small solid renal tumors are only detected on this phase. While many original reports have compared the AP with the VP, which delayed imaging sequence is most useful is still an unanswered question. One major advantage of image acquisition in the early EP is visualization of the collecting system and its relationship with central tumors, critical information if nephron-sparing surgery is to be considered. A recent study comparing VP and EP concluded that although VP images were more esthetically pleasing, both phases were equally effective in detecting and characterizing renal lesions (Yuh et al. 2000).

Fig. 3.4a,b. Small cyst in a 58-year-old man. **a** Axial contrast-enhanced CT scan in the VP clearly shows a small cyst (*arrow*) in the right kidney. **b** Axial contrast-enhanced CT scan in the AP shows that the cyst is much more subtle (*arrow*) and could be mistaken for the normal medulla.

3.3.2 Characterization of Renal Masses

Once a renal mass is detected, it is critical to accurately characterize it and to differentiate clinically insignificant renal cysts from solid and potentially malignant renal tumors. Renal cysts are fluid filled, and because they are avascular lesions, they demonstrate no enhancement after intravenous contrast administration. In contrast, RCC have a rich vascular supply and enhance significantly after contrast; thus, accurate measurement of the degree of enhancement in renal masses is critical to distinguish complex cysts from solid and potentially malignant lesions.

3.3.3 Concept of Significant Enhancement

Objective determination of lesion enhancement involves measurement of attenuation values within the mass before and after intravenous contrast. These quantitative data are obtained from operator-defined regions of interest (ROI) in various acquisitions sequences. Enhancement values of more than 10–12 Hounsfield units (HU) above pre-contrast measurements are considered significant. For these data to be reliable, it is important to pay careful attention to technical details, particularly when dealing with small lesions. The ROI should be placed in similar portions of the lesion, while all imaging parameters remain unchanged between the pre-contrast and post-contrast scans. If nodularity or wall thickening is present, their enhancement should be assessed. In small lesions, retrospective reconstruction over thinner intervals is helpful to avoid partial-volume averaging. Small cysts may demonstrate post-contrast "pseudo-enhancement" caused by beam-hardening artifacts, although this rarely exceeds the 10-HU threshold (Coulam et al. 2000).

In addition to these technical considerations, it is crucial to choose the optimal imaging sequence to measure the degree of enhancement. Most published studies agree that the VP or EP are more accurate than the AP in assessing the degree of enhancement of renal masses (Birnbaum et al. 1996; Kopka et al. 1997; Szolar et al. 1997; Yuh and Cohan 1999). Enhancement of solid renal tumors is time dependent and is greater in the VP compared with the AP. Some RCC enhance slowly over time and would be wrongly classified as non-enhancing if the AP were used.

Delayed scans can also be used in lieu of pre-contrast scans to characterize an incidental renal lesion detected on a routine contrast-enhanced CT. Macari and Bosniak (1999) have suggested that measurement of the washout of contrast in a lesion at 15 min allows differentiation between hyperdense cysts and renal neoplasms. In their study, there was no change in the attenuation of high-density cysts between the

initial contrast CT and the 15-min delayed images. In comparison, all lesions that proved to be neoplasms at surgery or on follow-up studies demonstrated decreased attenuation or "de-enhancement" of at least 15 HU on delayed CT, attributed to the washout of contrast from the vascular bed of the tumor (Macari and Bosniak 1999).

3.4 Renal Cystic Lesions

Renal cysts are among the most common renal lesions detected on cross-sectional imaging; the majority are isodense to water (attenuation values of <20 HU) and easily diagnosed, although some renal cysts do not fulfill the established diagnostic criteria and can prove difficult to define. Since its publication in 1986, the Bosniak classification of renal cysts has been widely used to classify these lesions and to separate cystic lesions that can be safely followed from those requiring surgical resection (Bosniak 1986; Curry et al. 2000):

1. Simple renal cysts. These cysts are classified as Bosniak category I, are homogeneous and isodense to water on pre-contrast images (<20 HU), do not enhance post-contrast, and display an imperceptible wall, a sharp interface with the adjacent renal parenchyma, and no septations or calcifications (Fig. 3.5). No further work-up or follow-up is necessary.
2. Minimally complicated cysts. These cysts belong to Bosniak category II, and contain one or two thin septa or thin wall calcifications, or may be hyperdense on pre-contrast images (homogeneously high attenuation; Figs. 3.6, 3.7). The wall is thin and they do not show enhancement post-contrast. These lesions are clearly benign and most are presumed to represent hemorrhagic cysts (Sussman et al. 1984). A separate category IIF includes lesions that are slightly more complex and require careful follow-up.
3. Indeterminate cystic lesions. These cysts comprise Bosniak category III and, although some prove benign at pathology, surgery is usually indicated because some RCC may be classified in this category. The cystic mass may be multilocular or may have thick septations or a uniformly thick wall or calcifications (Fig. 3.8).
4. Potentially malignant cystic masses. Lesions in Bosniak category IV are potentially malignant. The wall may be focally thick and enhancing, and enhancing nodules may be present within the mass or near the wall (Fig. 3.9).

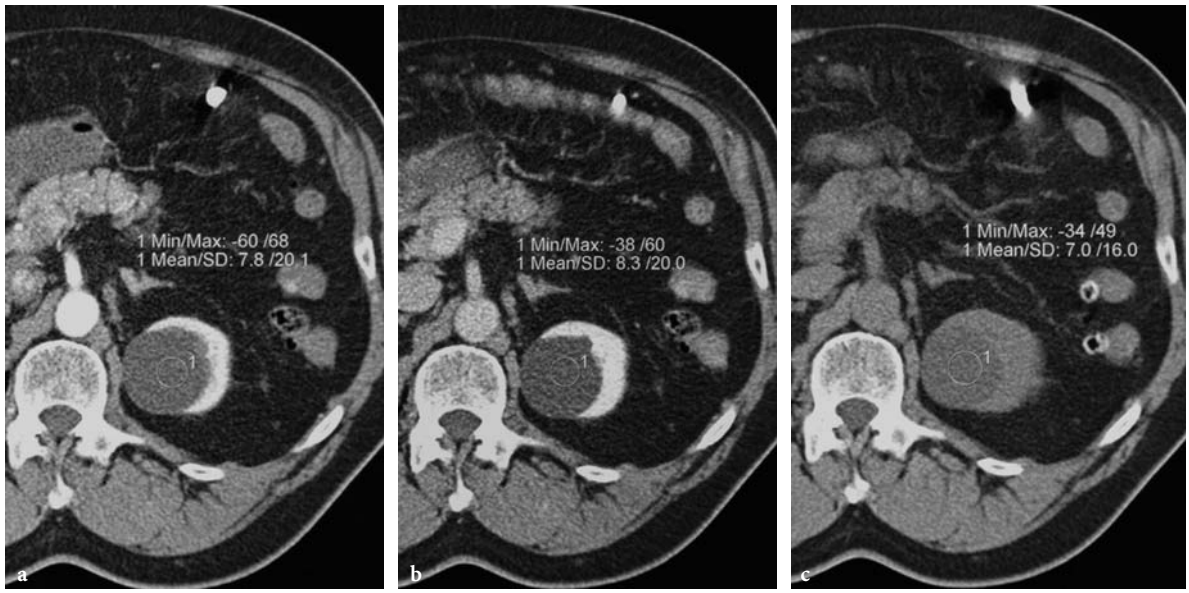

Fig. 3.5a-c. Simple renal cyst in a 65-year-old woman with an indeterminate left renal mass on ultrasound. **a** Axial precontrast CT scan shows a lesion in the left kidney. The lesion has water attenuation. **b** Axial contrast-enhanced CT scan in the AP shows no significant enhancement in the lesion. Note that the cyst has thin walls and no septation. **c** Axial contrast-enhanced CT scan in the EP confirms the absence of enhancement. This is a typical Bosniak I renal cyst.

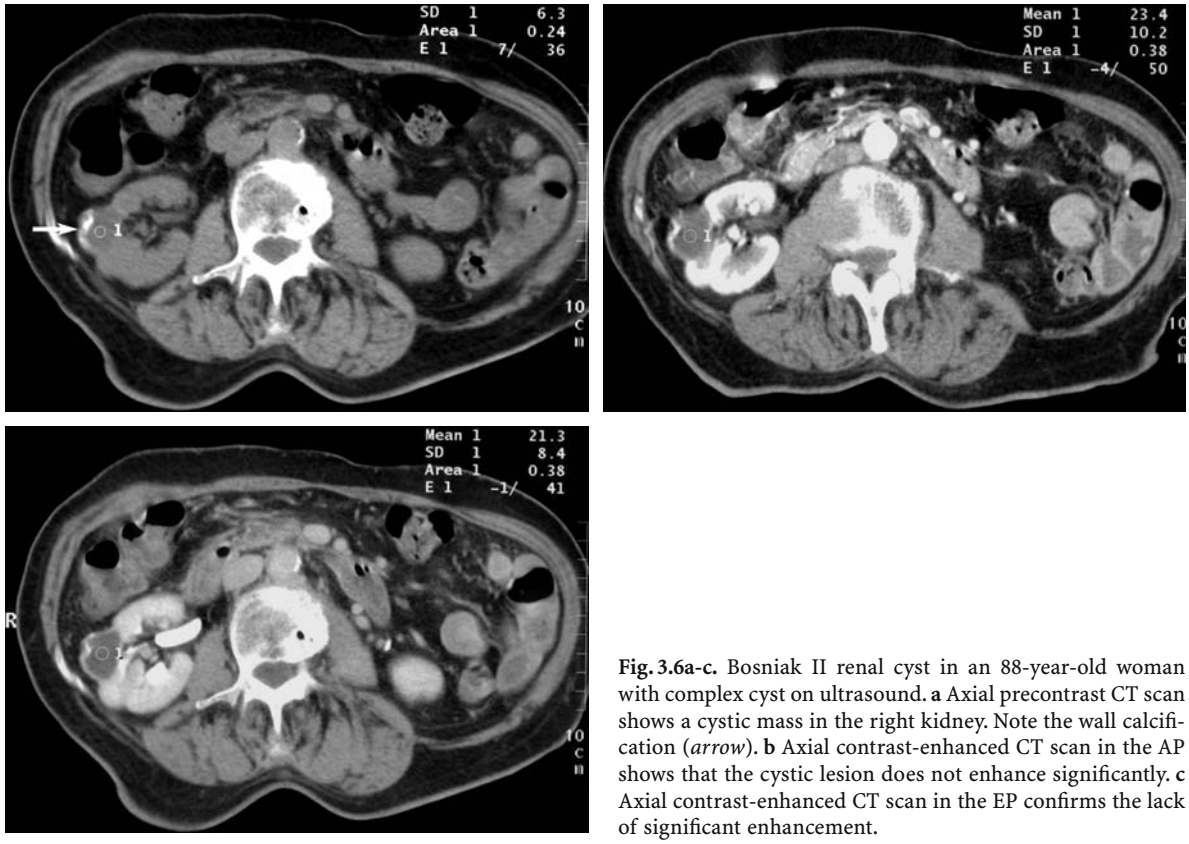

Fig. 3.6a-c. Bosniak II renal cyst in an 88-year-old woman with complex cyst on ultrasound. **a** Axial precontrast CT scan shows a cystic mass in the right kidney. Note the wall calcification (*arrow*). **b** Axial contrast-enhanced CT scan in the AP shows that the cystic lesion does not enhance significantly. **c** Axial contrast-enhanced CT scan in the EP confirms the lack of significant enhancement.

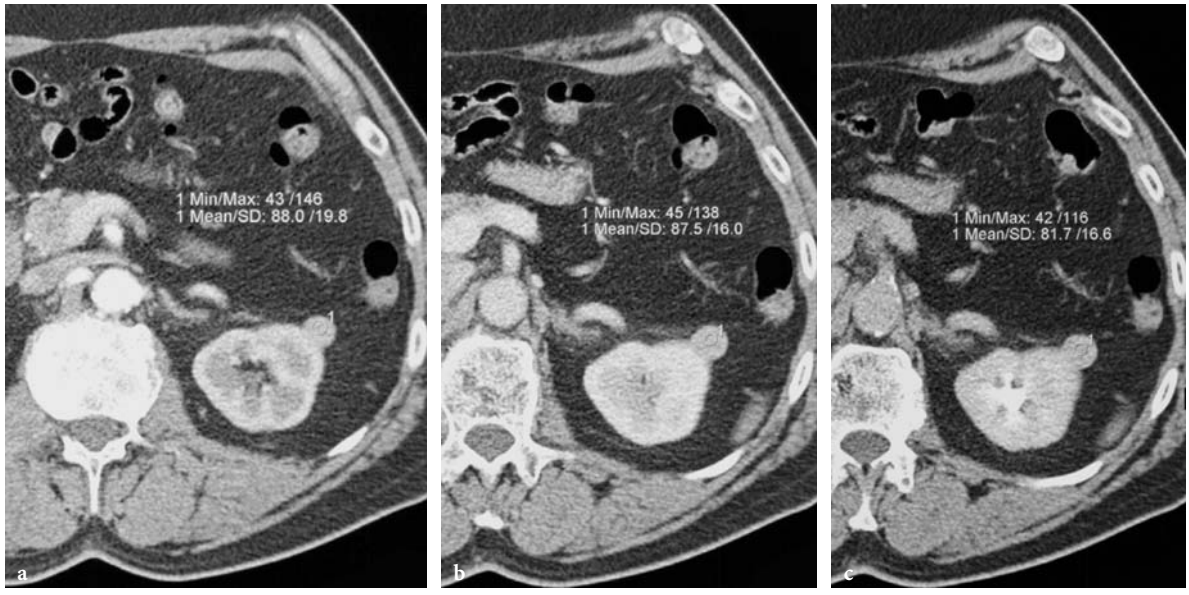

Fig. 3.7a-c. Incidental hyperdense cyst in a 60-year-old man. **a** Axial contrast-enhanced CT scan in the AP shows a hyperdense (88 HU) 1.5-cm exophytic lesion in the left kidney. **b** Axial contrast-enhanced CT scan in the VP shows no change in attenuation of the lesion. **c** Axial contrast-enhanced CT scan in the delayed phase shows no significant de-enhancement in the lesion (82 HU), confirming that this is a hyperdense cyst.

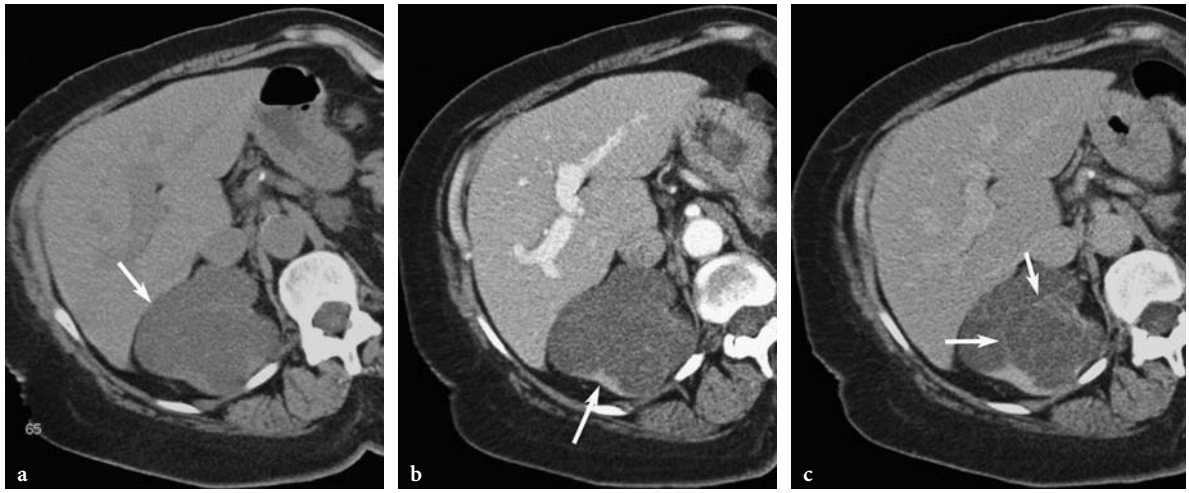

Fig. 3.8a-c. Bosniak III renal cyst in a 78-year-old woman. **a** Axial precontrast CT scan shows a cystic mass in the right kidney (*arrow*). **b** Axial contrast-enhanced CT scan in the AP shows enhancement in the wall (*arrow*). **c** Axial contrast-enhanced CT scan in the EP shows enhancement in the wall as well as thin, enhancing septations (*arrows*). The patient elected to "watch and wait" because of comorbid conditions. The lesion has been stable in size for 18 months.

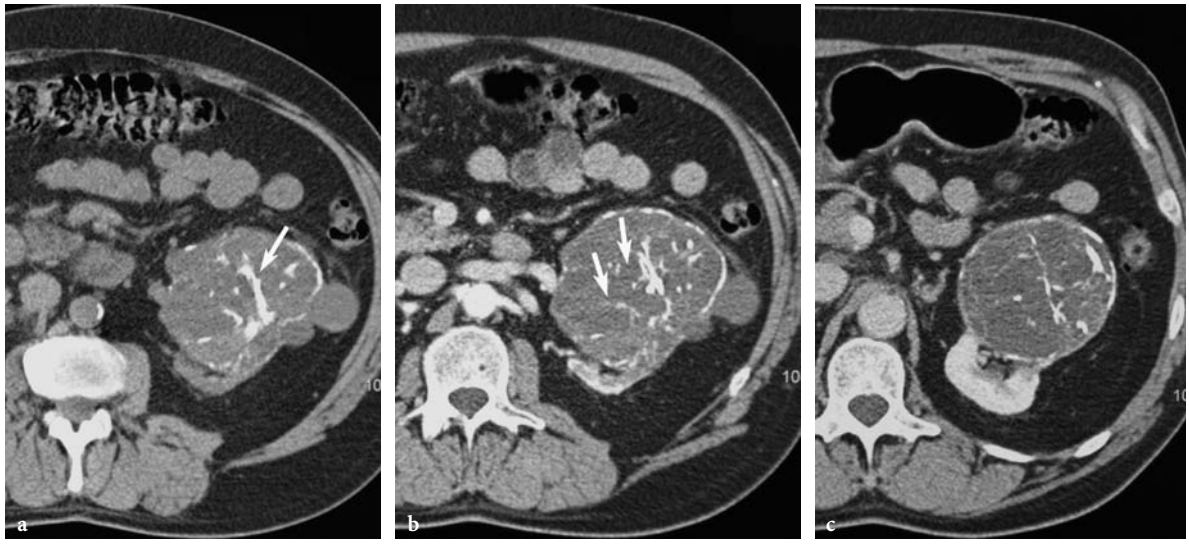

Fig. 3.9a-c. Incidental renal mass discovered on chest CT in a 68-year-old man. **a** Axial precontrast CT scan shows a 10-cm cystic mass with chunky calcifications in the left kidney (*arrow*). **b** Axial contrast-enhanced CT scan in the AP shows subtle areas of septal enhancement (*arrows*). Note that the left renal vein is normal. **c** Axial contrast-enhanced CT scan in the nephrographic phase (VP) shows similar findings. The patient underwent a radical left nephrectomy. Pathology revealed a cystic multilocular renal cell carcinoma, Fuhrman grade 2.

3.5 Renal Cell Carcinoma

3.5.1 Conventional Renal Cell Carcinoma

Conventional RCC arise from the convoluted tubules of the renal cortex and present as a solid expansile mass bulging and distorting the renal contour. They appear as a soft tissue mass, often of slightly higher attenuation than the normal renal parenchyma, with attenuation values of 20 HU or greater on precontrast CT. While the majority of RCC are solitary, approximately 5% are multifocal (Richstone et al. 2004). Small-to-moderate size RCC usually have well-defined margins due to the presence of

a pseudo-capsule formed by compressed surrounding renal tissue and fibrotic reaction. Calcifications are detected in up to 30% of tumors. After intravenous contrast, RCC exhibit significant enhancement above pre-contrast measurements, typically over 100 HU in the AP and 60 HU in the delayed phase (Figs. 3.10, 3.11). Small (3 cm or less) tumors usually have a homogenous appearance (Fig. 3.12) and show enhancement, whereas larger lesions tend to be more heterogeneous, due to intra-tumoral hemorrhage or necrosis. Another important finding recently described is that abnormal tumor vessels cause a relatively rapid washout of contrast from the tumor resulting in rapid de-enhancement (Macari and Bosniak 1999). This pattern is characteristic of the most common type of RCC, the conventional (or clear cell) tumor which accounts for approximately 70% of renal malignancies.

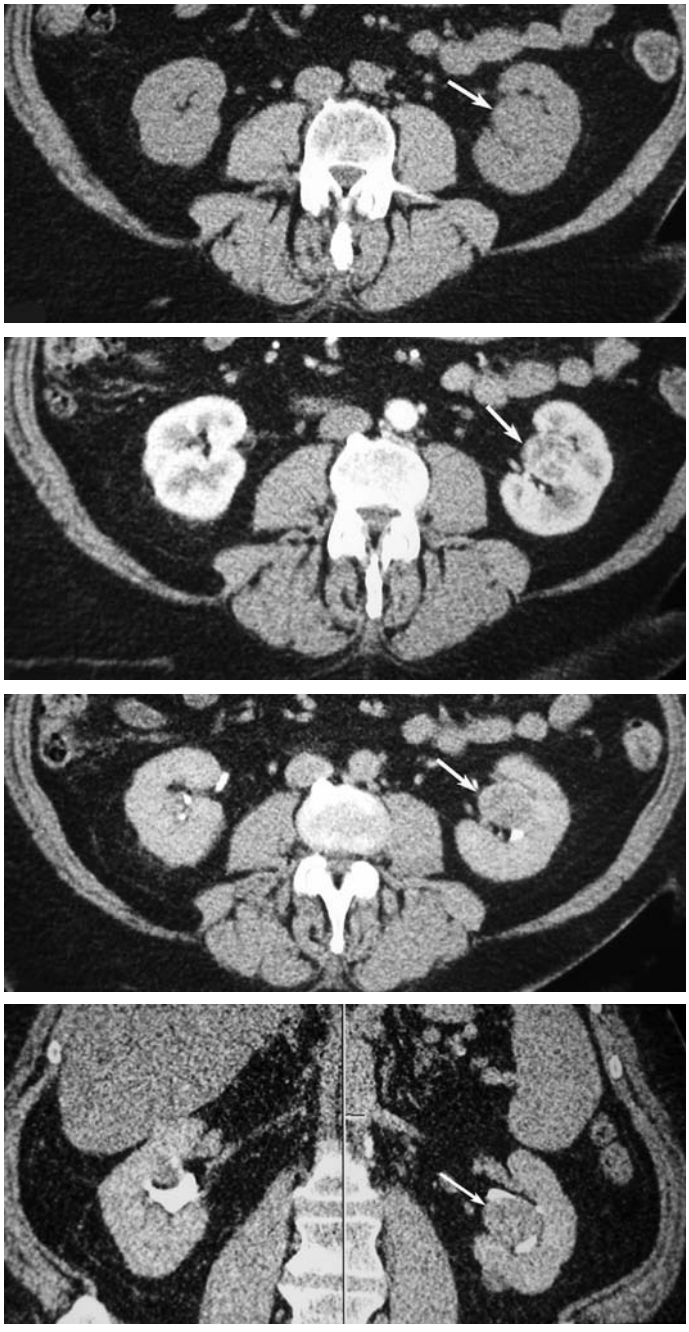

Fig. 3.10a-d. Small left renal cell carcinoma in a 61-year-old woman with history of partial right nephrectomy for renal cell carcinoma. **a** Axial unenhanced CT scan shows a 3-cm centrally located soft tissue mass (56 HU) in the left kidney (*arrow*). **b** Axial contrast-enhanced CT scan in the AP shows significant enhancement within the mass (98 HU; *arrow*). **c** Axial contrast-enhanced CT scan shows that the mass (63 HU; *arrow*) is distorting the collecting system. **d** Coronal-reconstruction CT image in the EP confirms the distortion of the collecting system by the mass (*arrow*). Although the location of the mass would favor a transitional cell carcinoma, its vascularity is suggestive of a renal cell carcinoma. A conventional renal cell carcinoma (Fuhrman grade 2) was found at nephrectomy.

a b c

Fig. 3.11a-c. Bilateral renal cell carcinomas in a 70-year-old man presenting with right upper quadrant pain. **a** Axial contrast-enhanced CT scan in the AP shows hypervascular masses in both kidneys (*arrows*). The mass in the left kidney extends into the renal hilum. **b** Axial contrast-enhanced CT scan in the VP shows the same findings (*arrows*). **c** Axial contrast-enhanced CT scan in the EP shows that the masses (*arrows*) are abutting the collecting system. Partial right and radical left nephrectomy revealed bilateral conventional renal cell carcinoma. (With permission from Sheth et al. 2001)

a b

Fig. 3.12a,b. Multiple small renal cell carcinomas in a 52-year-old man. **a** Axial contrast-enhanced CT scan in the AP shows multiple small homogeneously enhancing masses in the right kidney (*arrows*). **b** Axial contrast-enhanced CT scan in the VP shows that the masses (*arrows*) are hypodense to the normal renal parenchyma. Note that the smaller lesions are more clearly seen.

3.5.2
Papillary and Chromophobe Renal Cell Carcinoma

Papillary RCC are associated with a better prognosis, reaching 80–90% 5-year survival. They comprise about 20% of RCC. Chromophobe cancers have the most favorable outcome with over 90% 5-year survival. By contrast, the rare (<1% of renal cell cancers) collecting duct carcinoma is associated with the worst prognosis with 5-year mortality reaching 95%. In a recently published retrospective review, Kim et al. (2002) attempted to determine whether CT appearance and enhancement patterns correlated with the histological type of tumor. In their study, degree of enhancement was the most useful parameter. Most conventional carcinomas enhanced strongly in the AP and delayed phases and large masses were heterogeneous. By contrast, chromophobe tumors showed weak and homogeneous enhancement. Papillary cancers tend to exhibit a more gradual enhancement (Figs. 3.13, 3.14; Jinzaki et al. 2000).

3.5.3
Collecting Duct Cancer

Collecting duct carcinomas are rare, aggressive cancers presumably arising from the collecting ducts of Bellini in the renal medulla. Tumor growth follows an infiltrative pattern, with the underlying normal renal tissues used as scaffolding for the invasive growth. This diagnosis can be suggested on CT, if the tumor is centered in the medullary portion of the kidney and infiltrates the renal parenchyma, with poorly defined transition and preservation of the reniform shape of the kidney (Pickhardt et al. 2001). The prognosis is poor.

3.6
Differential Diagnosis of Solid Renal Masses

Careful analysis of CT appearance and attenuation values is often useful in differentiating RCC from other benign or malignant renal tumors; however, if imaging findings are equivocal, image-guided percutaneous biopsy is invaluable in achieving the correct diagnosis (Neuzillet et al. 2004).

3.6.1
Benign Renal Tumors

3.6.1.1
Renal Oncocytoma

Renal oncocytomas are histologically benign solid vascular neoplasms of the kidney. They vary in size

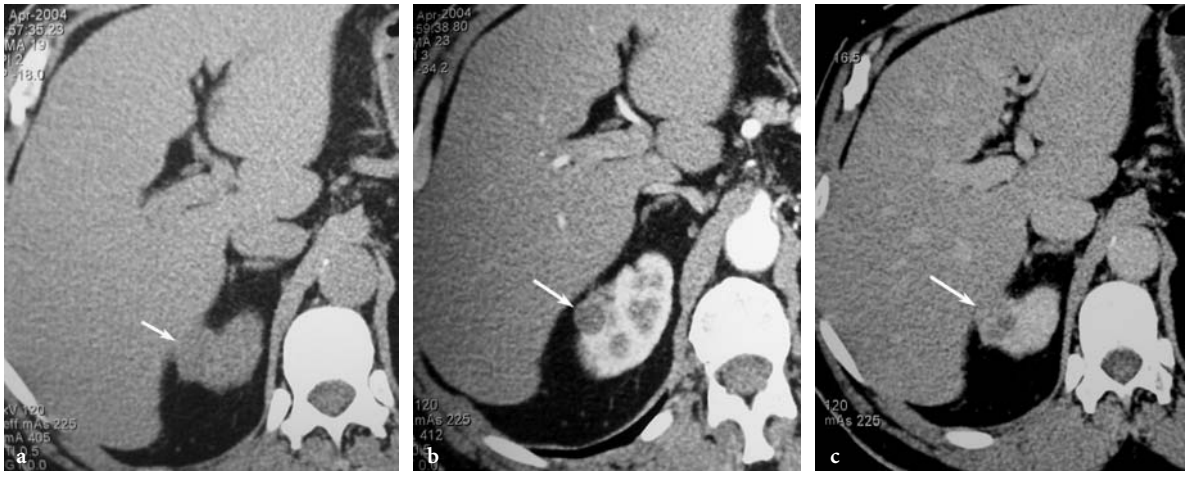

Fig. 3.13a-c. Incidental renal cell carcinoma in a 62-year-old man with history of staghorn calculus. **a** Axial precontrast CT scan shows a 2.5-cm exophytic soft tissue mass (*arrow*) in the upper pole of the right kidney. Region of interest (ROI) reading was 33.3 HU. **b** Axial contrast-enhanced CT scan in the AP shows the mass (*arrow*). The ROI reading was 33.6 HU. **c** Axial contrast-enhanced CT scan in the early EP shows enhancement within the mass (*arrow*). The ROI reading was 73.2 HU. Partial right nephrectomy revealed a papillary renal cell carcinoma.

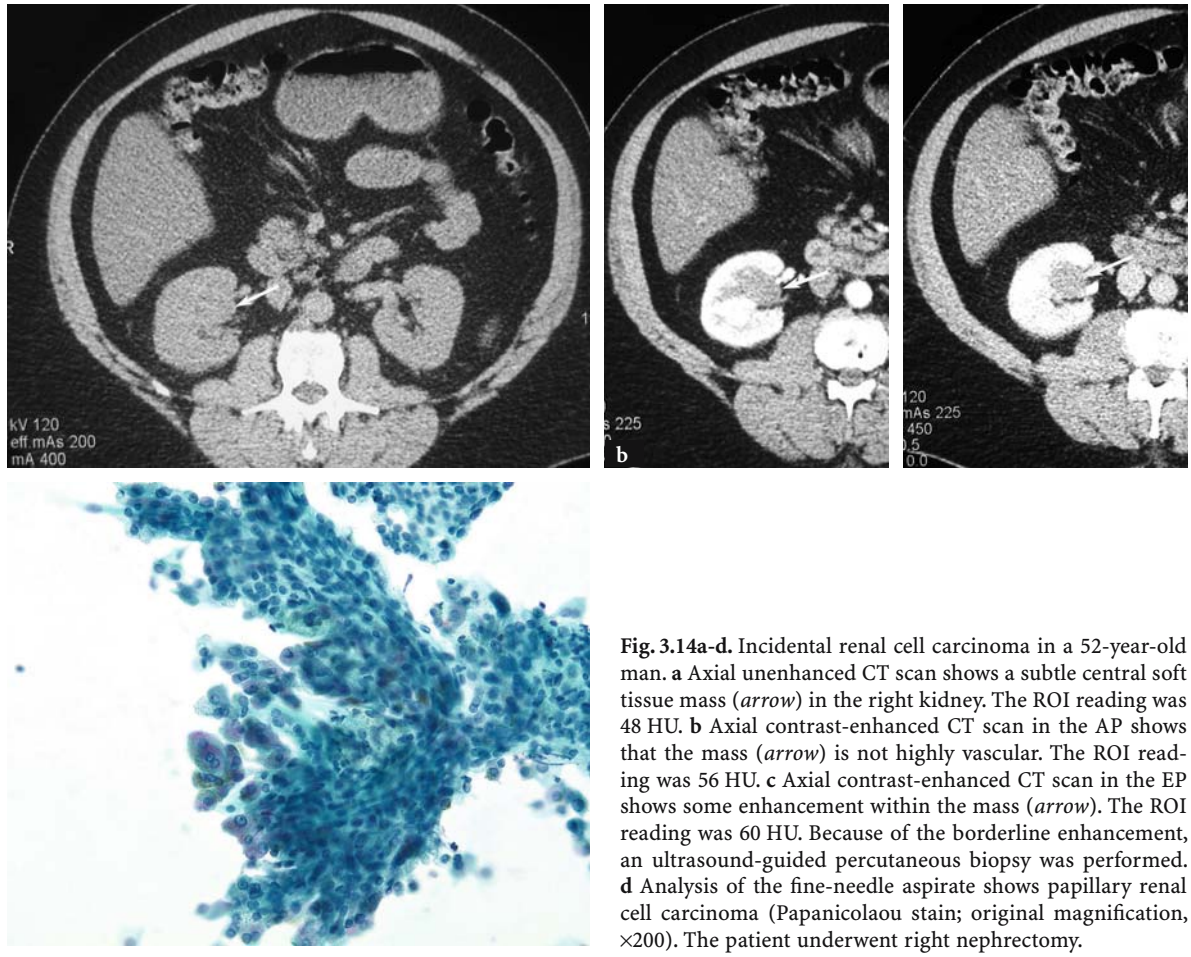

Fig. 3.14a-d. Incidental renal cell carcinoma in a 52-year-old man. **a** Axial unenhanced CT scan shows a subtle central soft tissue mass (*arrow*) in the right kidney. The ROI reading was 48 HU. **b** Axial contrast-enhanced CT scan in the AP shows that the mass (*arrow*) is not highly vascular. The ROI reading was 56 HU. **c** Axial contrast-enhanced CT scan in the EP shows some enhancement within the mass (*arrow*). The ROI reading was 60 HU. Because of the borderline enhancement, an ultrasound-guided percutaneous biopsy was performed. **d** Analysis of the fine-needle aspirate shows papillary renal cell carcinoma (Papanicolaou stain; original magnification, ×200). The patient underwent right nephrectomy.

from less than 1 cm to 15–20 cm. Although traditionally they have rarely been diagnosed before nephrectomy, preoperative diagnosis is desirable, as less aggressive surgery, such as enucleation or partial nephrectomy, is the preferred treatment. The CT appearance of a homogeneously enhancing large mass with a pseudo-capsule and a central scar should suggest the oncocytoma, since large RCC tend to enhance heterogeneously (Fig. 3.15). Small oncocytomas cannot be reliably distinguished from RCC with imaging (Fig. 3.16). With current improvements in cytopathological techniques, percutaneous biopsy can be useful in differentiating oncocytomas from RCC by demonstrating large eosinophilic epithelial cells with mitochondria rich cytoplasm, but there is significant overlap with renal cell cancer with oncocytic features (Liu and Fanning 2001).

3.6.1.2 Renal Angiomyolipoma

Angiomyolipomas are benign renal hamartomatous tumors composed of varying amounts of mature adipose tissue, smooth muscle, and abnormal blood vessels. Solitary angiomyolipomas are usually sporadic, whereas multiple lesions are part of the spectrum of renal abnormalities associated with tuberous sclerosis. Many of these tumors are small and detected serendipitously. On the other hand, large angiomyolipomas can hemorrhage and present acutely. In many cases a specific diagnosis can easily be established on CT by demonstrating even a small amount of fat within the lesion (Figs. 3.17, 3.18). Computed tomography can also detect intra- or perirenal blood as well as perinephric extension of angiomyolipomas (Sherman et al. 1981).

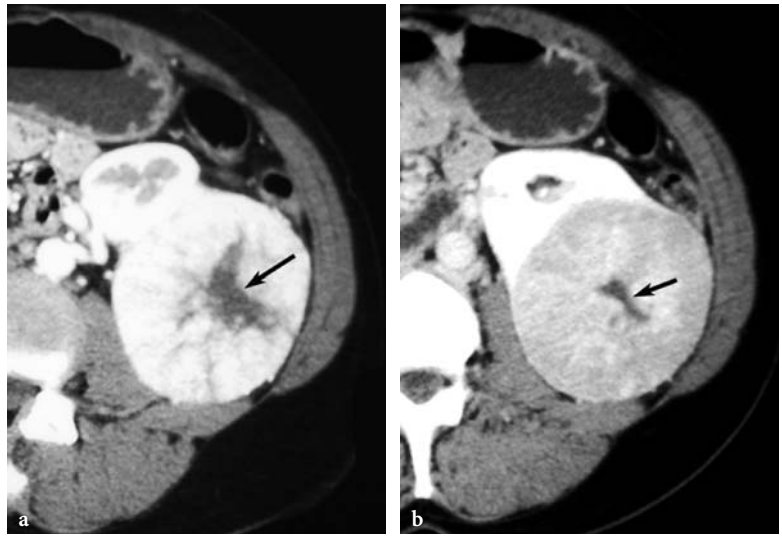

Fig. 3.15a,b. Incidental oncocytoma in a 45-year-old woman. **a** Axial contrast-enhanced CT scan in the AP shows a large hypervascular mass in the left kidney. Note that the tumor is enhancing homogeneously and has a central scar (*arrow*). **b** Axial contrast-enhanced CT scan in the VP shows that the mass central scar is well depicted (*arrow*). Partial left nephrectomy was performed and pathology revealed an oncocytoma.

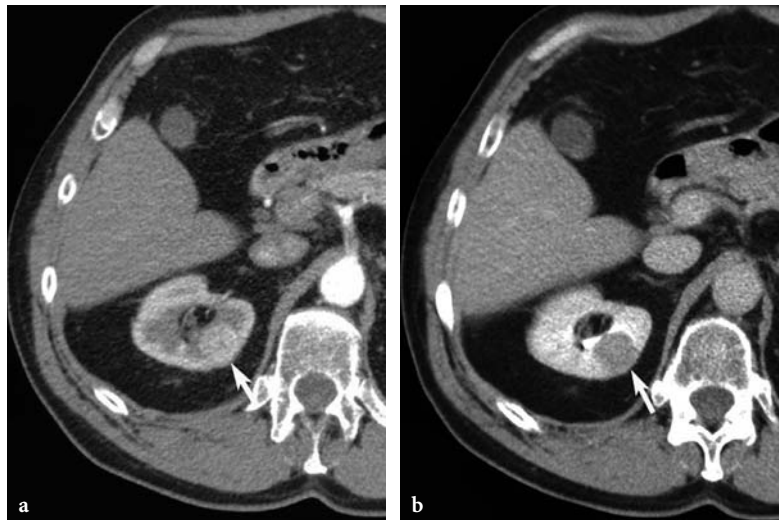

Fig. 3.16a,b. Incidental oncocytoma in a 70-year-old man. **a** Axial contrast-enhanced CT scan in the AP shows a subtle 2-cm hypervascular mass (*arrow*). **b** Axial contrast-enhanced CT scan in the VP shows that the mass (*arrow*) is better visualized because of the enhancing normal renal parenchyma. The patient underwent laparoscopic nephrectomy and pathology revealed a 3-cm oncocytoma.

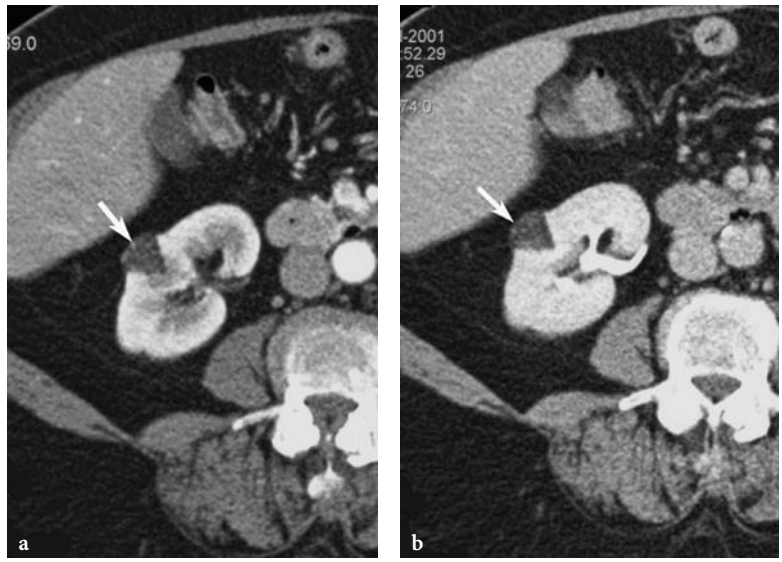

Fig. 3.17a,b. Incidental small angiomyolipoma in a 54-year-old woman. **a** Axial contrast-enhanced CT scan in the AP shows a 3-cm cortical mass (*arrow*) in the right kidney. The mass is of fat density. This is a typical appearance for an angiomyolipoma and no further evaluation is necessary. **b** Axial contrast-enhanced CT scan in the EP confirms the diagnosis (*arrow*).

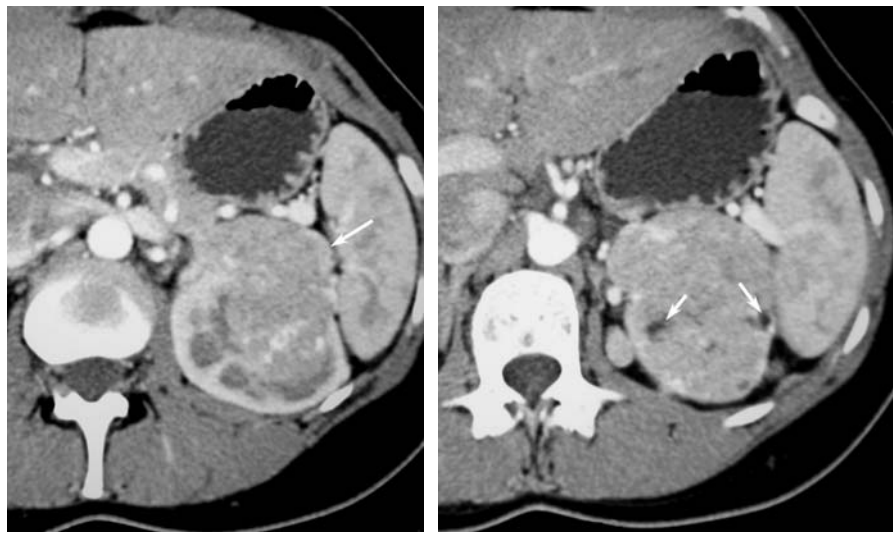

Fig. 3.18a,b. Angiomyolipoma with small amount of fat in a 37-year-old woman with history of left flank pain and previous bleed. **a** Axial contrast-enhanced CT scan in the AP shows a 6-cm vascular soft tissue mass in the left kidney (*arrow*). **b** Axial contrast-enhanced CT scan in the AP shows a small amount of fat (*arrows*) within the mass, indicating that this is most likely an angiomyolipoma. The patient underwent a successful partial left nephrectomy. The diagnosis of angiomyolipoma was confirmed at pathology.

Approximately 4.5% of angiomyolipomas contain only a minimal amount of fat that is below the detection threshold of CT (Kim et al. 2004), and they cannot be readily differentiated from RCC (Sant et al. 1984). The CT findings suggestive of angiomyolipomas with minimal fat include homogeneous high attenuation on pre-contrast scans, and homogeneous enhancement post-contrast scans (Jinzaki et al. 1997). Kim et al. (2004) suggest that prolonged lesion enhancement, defined as tumor attenuation values at least 20 HU higher in the excretory phase than in the corticomedullary phase, can help the differential diagnosis. In equivocal cases percutaneous biopsy is useful (Sant et al. 1990).

3.6.2 Malignant Renal Tumors Other Than Renal Cell Carcinoma

3.6.2.1 Intrarenal Transitional Cell Carcinoma

When transitional cell carcinoma spreads to the renal parenchyma, it presents as a centrally located infiltrating mass invading the renal sinus fat with poorly defined borders and lower enhancement than the normal renal parenchyma (Fig. 3.19; Bree et al. 1990; Fukuya et al. 1994; Igarashi et al. 1994). These tumors tend to be aggressive, with high-grade histology. Loco-regional and distant metastases are common and the prognosis is poor.

3.6.2.2 Renal Metastases and Lymphoma

Metastases are the most common malignant lesions found in the kidneys at autopsy (Hietala and Wahlqvist 1982). They reach the renal cortex via hematogenous spread and are generally asymptomatic. The most common primary cancers metastasizing to the kidneys include lung and breast cancers followed by melanoma and gastric carcinoma (Bailey et al. 1998). In the oncological population, routine contrast CT images are usually obtained in the venous phase of enhancement. Renal metastases are easily diagnosed if multiple bilateral renal cortical lesions enhance less than the surrounding normal kidney; however, an increasing number of incidental small RCC are being detected on routine surveillance CT in patients with an extra-renal malignancy. In this population the finding of a solitary renal mass warrants image-guided biopsy to determine appropriate management.

The genitourinary tract is the most common location for spread of non-Hodgkin lymphoma, after the hematopoietic and reticuloendothelial system. A detailed discussion of the CT appearance of renal lymphoma is provided in Chapter 18.

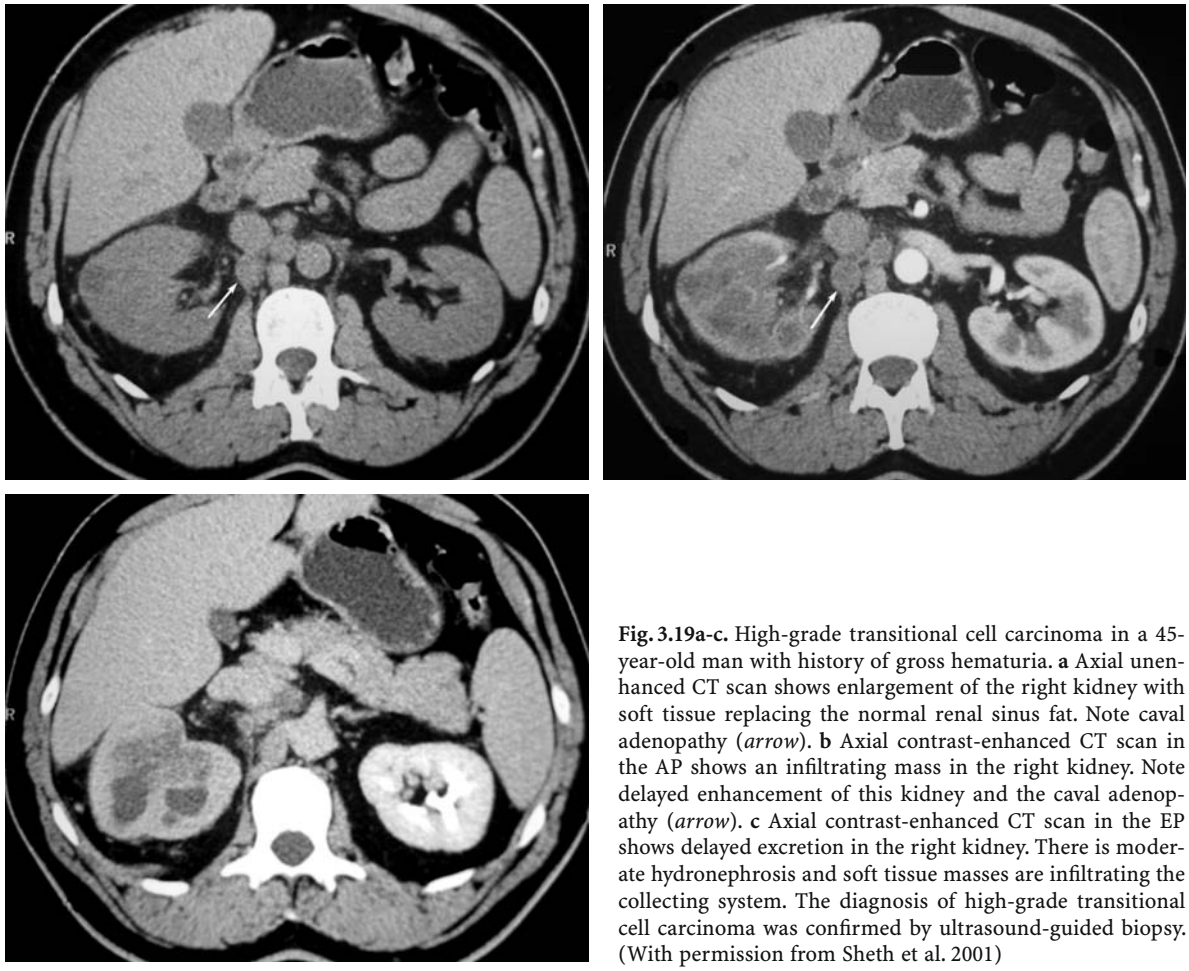

Fig. 3.19a-c. High-grade transitional cell carcinoma in a 45-year-old man with history of gross hematuria. **a** Axial unenhanced CT scan shows enlargement of the right kidney with soft tissue replacing the normal renal sinus fat. Note caval adenopathy (*arrow*). **b** Axial contrast-enhanced CT scan in the AP shows an infiltrating mass in the right kidney. Note delayed enhancement of this kidney and the caval adenopathy (*arrow*). **c** Axial contrast-enhanced CT scan in the EP shows delayed excretion in the right kidney. There is moderate hydronephrosis and soft tissue masses are infiltrating the collecting system. The diagnosis of high-grade transitional cell carcinoma was confirmed by ultrasound-guided biopsy. (With permission from Sheth et al. 2001)

3.7 Role of CT in Staging of Renal Cell Carcinoma

Accurate staging at the time of diagnosis is essential for determining prognosis and formulating a therapeutic plan. In 2004, multidetector CT remains the most widely available and single most effective modality for staging patients with RCC, with reported accuracy of 80–95% (Catalano et al. 2003; Hallscheidt et al. 2004; Johnson et al. 1987; Sheth et al. 2001).

Numerous studies have shown that the anatomic extent of the tumor at the time of diagnosis is the single most important factor in determining prognosis (Dinney et al. 1992; Thrasher and Paulson 1993). Disease-free survival is inversely correlated with increasing pathological stage, falling from 60 to 90% 5-year survival for patients with organ confined lesions to 5–10% for those with distant metastases.

The TNM classification, which defines the anatomic extent of the tumor more precisely, has gained wide acceptance and is progressively replacing the older Robson classification.

3.7.1 Tumors Confined Within the Renal Capsule

Patients with RCC confined to the kidney have the best prognosis with 5-year survival rates of 60–90% following nephrectomy (Fig. 3.20; Thrasher and Paulson 1993). Many of these tumors are detected incidentally on cross-sectional imaging performed for unrelated indications. The recent modification of the TNM classification separating tumors 7 cm or less in size (stage T1) from lesions larger than 7 cm (stage T2) reflects the impact of tumor size on survival (Russo 2000).

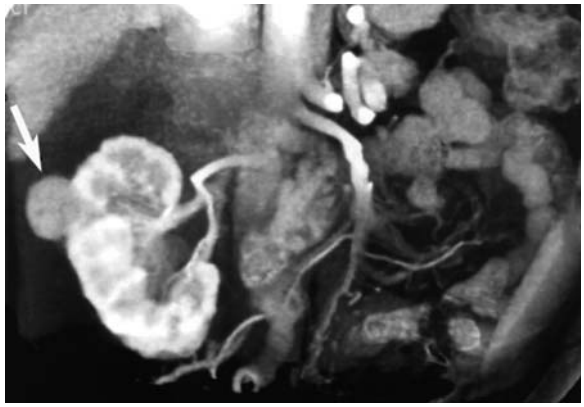

Fig. 3.20. Incidental renal cell carcinoma in a 62-year-old man. Coronal oblique plane 3D CT image in AP shows that the tumor measures 3 cm and is peripheral and exophytic (*arrow*). This is a stage T1 lesion. This tumor is in an ideal location for nephron-sparing surgery, which was performed successfully.

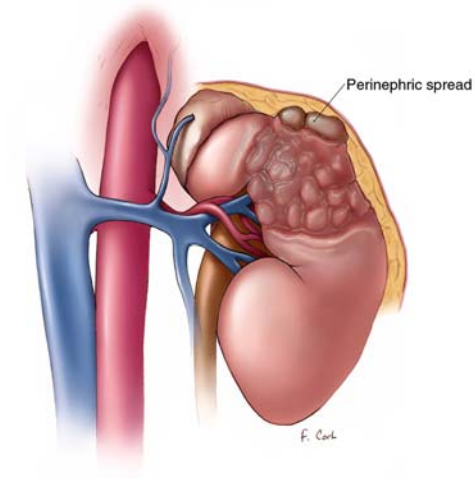

Fig. 3.21. Perinephric spread of renal cell carcinoma. (With permission from Sheth et al. 2001)

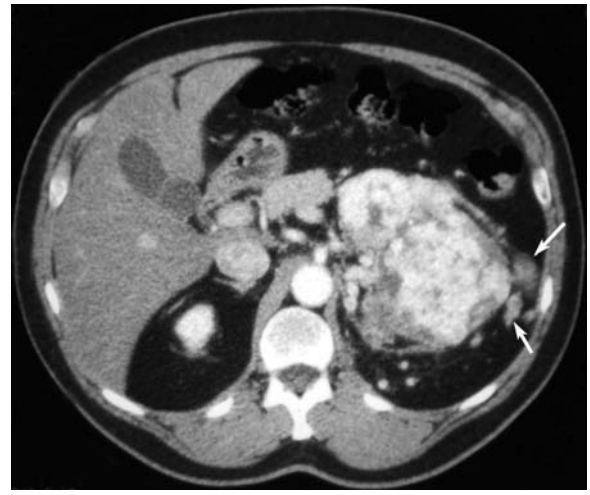

Fig. 3.22. Large renal cell carcinoma with perinephric tumor spread in a 65-year-old man with hematuria. Axial contrast-enhanced CT scan in the AP shows a large hypervascular mass in the left kidney. Several soft tissue nodules seen in the perinephric space indicate spread of tumor (*arrows*). The pathological stage of tumor was confirmed to be T3a at nephrectomy. (With permission from Sheth et al. 2001)

3.7.2 Perinephric Spread of Tumor

Under- and over-staging of perinephric invasion is the most common cause of staging errors on CT (Catalano et al. 2003; Johnson et al. 1987; Kopka et al. 1997). The presence of a pseudo-capsule suggests that the tumor is confined to the kidney (Catalano et al. 2003). The most specific finding of stage T3a disease is the presence of an enhancing nodule in the perinephric space (Figs. 3.21, 3.22; Johnson et al. 1987). Tumor spread within the perinephric fat cannot always be reliably diagnosed, and differentiation between stage T2 and stage T3a tumors is problematic. Perinephric stranding does not reliably indicate tumor spread and is also found in about half of patients with localized T1 and T2 tumors. In these patients, perinephric stranding may be caused by edema, vascular engorgement of previous inflammation.

Diagnosis of perinephric extension has important prognostic as well as therapeutic implications, as T3a tumors are best treated with radical nephrectomy.

3.7.3 Imaging of the Ipsilateral Adrenal Gland

The incidence of adrenal metastases is low, reported as 4.3% in one large series (Sagalowsky et al. 1994). Evaluation of the adrenal gland is important for surgical management because the current trend is to spare the ipsilateral adrenal gland unless an abnormality is suggested on CT. In one study of 157 patients with RCC who underwent radical nephrectomy, visualization of a normal adrenal gland on CT was associated with a 100% negative predictive value for tumor spread to the gland at pathology (Sagalowsky et al. 1994). By contrast, adrenal enlargement, displacement, or non-visualization were associated with malignant spread in 24% of cases, which indicates that adrenalectomy should be performed (Ramani et al. 2003; Sagalowsky et al. 1994).

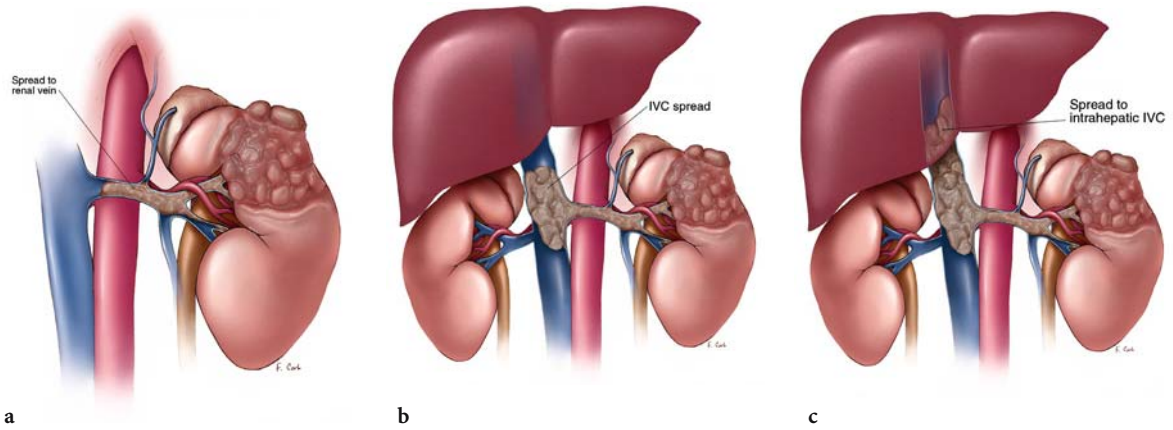

Fig. 3.23a-c. Venous spread of renal cell carcinoma. **a** Tumor spread limited to the renal vein (stage T3b). **b** Tumor spread into the inferior vena cava, infrahepatic (stage T3c). **c** Tumor spread into the inferior vena cava, hepatic (stage T3c). (With permission from Sheth et al. 2001)

3.7.4 Venous Spread of Tumor

Because RCC has a propensity to extend into the venous system, accurate preoperative evaluation of the renal vein and inferior vena cava is crucial. Extension of RCC limited to the renal vein (stage T3b) occurs in approximately 23% of patients and does not adversely affect the prognosis (Fig. 3.6; Russo 2000). Spread of the tumor into the inferior vena cava is found in 4–10% of patients and is more common with right-side lesions (Kallman et al. 1992). Patients with extensive IVC involvement and with nodal or distant metastases carry a relatively good prognosis with 5-year survival of 32–64%, provided that the thrombus is intraluminal, does not invade the vessel wall, and can be entirely resected (Staehler and Brkovic 2000). In these patients aggressive surgical resection with curative intent is justified (Fig. 3.24).

Helical CT has been shown to be highly accurate for diagnosing spread of RCC into the renal vein, with reported accuracy reaching 100% (Catalano et al. 2003). The most specific sign of venous extension is the presence of a low-density filling defect within the vein (Zeman et al. 1988). An abrupt change in the caliber of the renal vein or the presence of a clot within collateral veins are helpful ancillary signs.

The CT appearance of the thrombus helps distinguish malignant from bland thrombus. Heterogeneous enhancement of the thrombus with contrast indicates neovascularity, and thus, tumor thrombus (Fig. 3.24). Direct continuity of the thrombus with the primary tumor suggests tumor thrombus.

If tumor spread is identified within the IVC, precise delineation of the superior extent of the thrombus is essential for the surgeon to plan the optimal surgical strategy for thrombectomy and minimize the risk of intraoperative tumor embolism (Kallman et al. 1992; Staehler and Brkovic 2000; Suggs et al. 1991). The level of IVC involvement dictates the surgical approach. If the thrombus remains infrahepatic, it can be resected via an abdominal incision. If extension is detected to the level of the retrohepatic IVC, a right thoraco-abdominal approach allows access to the suprahepatic IVC.

3.7.5 Regional Lymph Node Metastases

The presence of regional lymph node metastases carries a poor prognosis with reported 5-year survival rates of 5–30% (Fig. 3.25; Thrasher and Paulson 1993). The CT diagnosis of lymph node metastases relies on nodal enlargement above 1 cm short-axis diameter. This criterion was associated with a 4% false-negative rate in a series of 163 patients with RCC who underwent nephrectomy and regional lymph node dissection. This study also showed that in more than half of the patients, nodal enlargement was caused by benign inflammatory changes. This reactive nodal enlargement is often associated with extensive tumor necrosis or venous thrombosis and may represent a reactive immune response (Russo 2000; Studer et al. 1990). Nodal enlargement demonstrated on CT should not disqualify patients for nephrec-

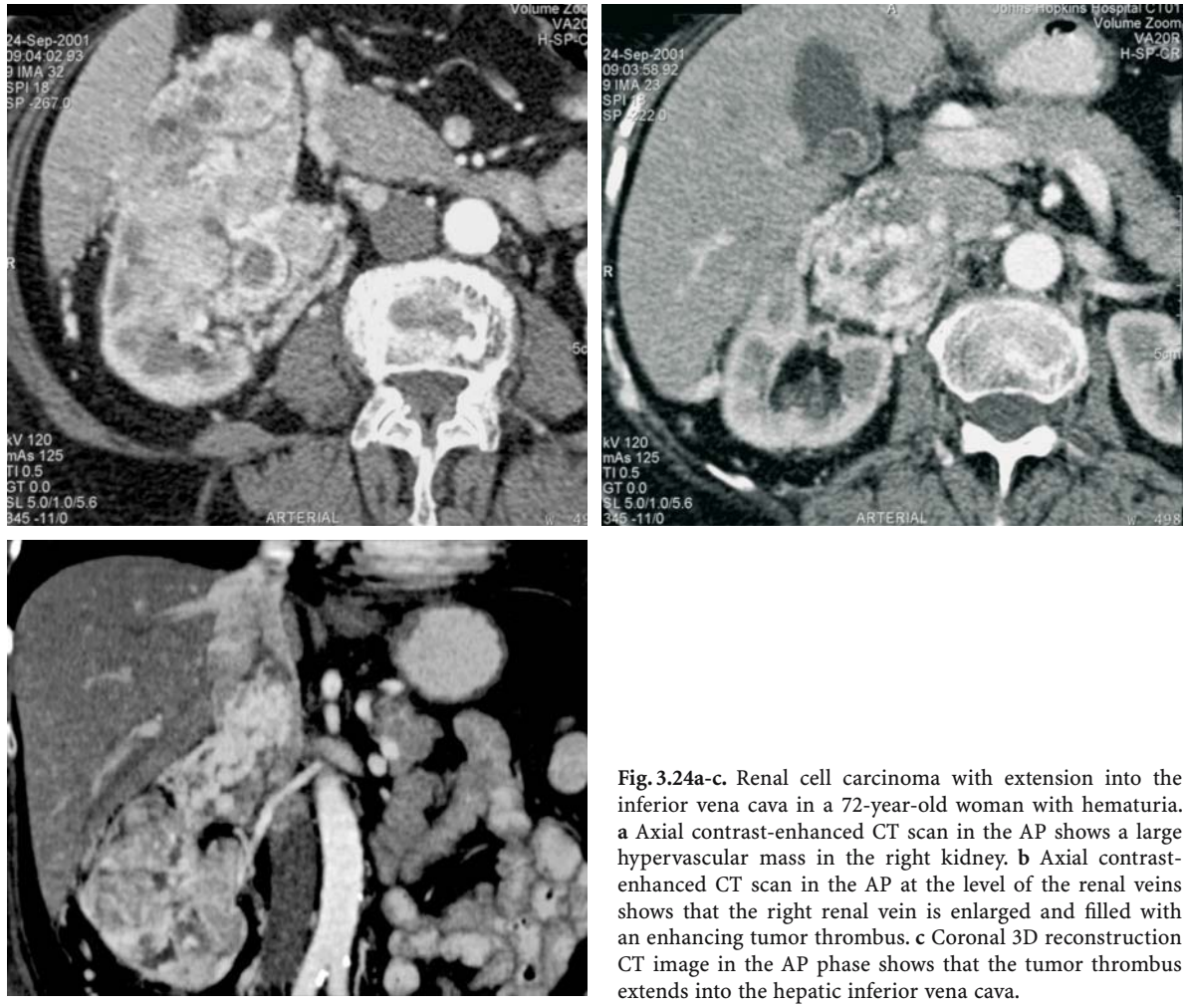

Fig. 3.24a-c. Renal cell carcinoma with extension into the inferior vena cava in a 72-year-old woman with hematuria. **a** Axial contrast-enhanced CT scan in the AP shows a large hypervascular mass in the right kidney. **b** Axial contrast-enhanced CT scan in the AP at the level of the renal veins shows that the right renal vein is enlarged and filled with an enhancing tumor thrombus. **c** Coronal 3D reconstruction CT image in the AP phase shows that the tumor thrombus extends into the hepatic inferior vena cava.

tomy unless metastatic spread is confirmed with fine-needle aspiration. The enhancement pattern within the node may also help differentiate reactive from malignant adenopathy: metastatic nodes may enhance, particularly if the primary tumor is very vascular (Fig. 3.25).

3.7.6 Local Extension and Distant Metastases

Direct extension of RCC outside Gerota's fascia into neighboring organs (stage T4a) is difficult to diagnose with certainty unless there is a demonstrable focal change in attenuation within the adjacent organ. Loss of tissue planes and irregular margins between the tumor and surrounding structures raise the possibility of direct infiltration, but can be seen in up to 15% of cases without surgically confirmed stage T4a disease (Johnson et al. 1987). Three-dimensional CT displays the tumor and its relationship to the adjacent organs in multiple planes and orientations and is very valuable in difficult cases to increase diagnostic confidence and help plan surgical resection (Catalano et al. 2003; Hallscheidt et al. 2004; Sheth et al. 2001).

Renal cell carcinoma metastasizes most frequently to the lungs and mediastinum, bones, and liver. Less common sites include the contralateral kidney, the adrenal gland, the brain, pancreas, mesentery, and abdominal wall (Dinney et al. 1992; Thrasher and Paulson 1993). Like the primary tumor, metastatic lesions tend to be hypervascular. The prognosis for these patients is dismal, with reported 5-year survival of 5–10%; however, patients with a solitary metastasis may benefit from aggressive management with nephrectomy and surgical removal of the metastatic lesion.

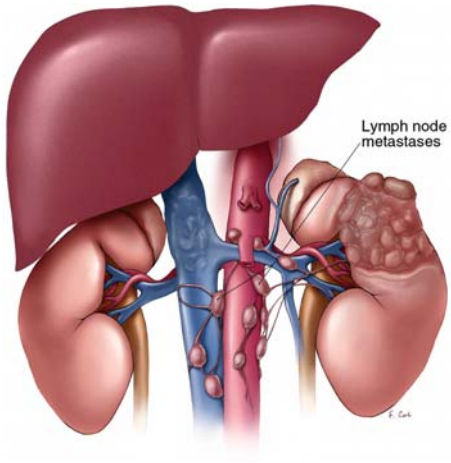

Fig. 3.25. Renal cell carcinoma with regional lymph node metastases. (With permission from Sheth et al. 2001)

Fig. 3.26. Renal cell carcinoma with regional lymph node metastases in a 66-year-old man with hematuria. Axial contrast-enhanced CT scan in the AP shows hypervascular mass in the left kidney with hypervascular left para-aortic node (*arrow*).

3.8 Role of CT in Planning for Nephron-Sparing Surgery

In the past 20 years, the clinical presentation of RCC has evolved. The widespread use of cross-sectional imaging techniques has led to a dramatic increase in the number of incidentally discovered tumors. These asymptomatic tumors, which now comprise 25 to almost 50% of all surgically treated RCC, are generally confined to the renal capsule, relatively small in size (4–5 cm or less), and associated with an excellent prognosis following surgical removal.

These changes in the presentation of RCC have stimulated a growing trend towards nephron-sparing surgical techniques (Novick 1992; Thrasher et al. 1994). Nephron-sparing surgery entails complete excision of the renal tumor with a margin of at least 0.5 cm of normal renal tissue while preserving the largest amount of functioning renal parenchyma. It is the treatment of choice when radical nephrectomy would render the patient anephric with subsequent need for dialysis. Nephron-sparing surgery is also being increasingly advocated for the treatment of small RCC as current data show survival rates comparable to radical nephrectomy (Herr 1999).

Three-dimensional CT helps delineate the precise location of the renal mass, its relationship to the surface of the kidney, the collecting system, and the renal vessels. The arterial and venous anatomy of the kidney is depicted on the 3D CT angiogram (Smith et al. 1999). The most suitable lesion for nephron-sparing surgery is small in diameter (<4 cm), polar, cortical, and far from the renal hilum and collecting system (Fig. 3.20).

3.9 Conclusion

With the advent of MDCT, the role of CT in the diagnosis and pre-surgical planning of RCC has been greatly expanded. Along with these technical improvements, new challenges facing the radiologist have emerged. These challenges include the adoption of scanning protocols designed to maximize diagnostic accuracy while at the same time minimizing radiation to the patient and image overload for the radiologist. Renal CT with multiple-phase image acquisitions as well as 3D reconstructions provides the clinician with all the information necessary for surgical planning.

References

Bailey JE, Roubidoux MA, Dunnick NR (1998) Secondary renal neoplasms. Abdom Imaging 23:266–274

Birnbaum BA, Jacobs JE, Ramchandani P (1996) Multiphasic renal CT: comparison of renal mass enhancement during the corticomedullary and nephrographic phases. Radiology 200:753–758

Bosniak MA (1986) The current radiological approach to renal cysts. Radiology 158:1–10
Bree RL, Schultz SR, Hayes R (1990) Large infiltrating renal transitional cell carcinomas: CT and ultrasound features. J Comput Assist Tomogr 14:381–385
Carrim ZI, Murchison JT (2003) The prevalence of simple renal and hepatic cysts detected by spiral computed tomography. Clin Radiol 58:626–629
Catalano C, Fraioli F, Laghi A, Napoli A, Pediconi F, Danti M, Nardis P, Passariello R (2003) High-resolution multidetector CT in the preoperative evaluation of patients with renal cell carcinoma. Am J Roentgenol 180:1271–1277
Cohan RH, Sherman LS, Korobkin M, Bass JC, Francis IR (1995) Renal masses: assessment of corticomedullary-phase and nephrographic-phase CT scans. Radiology 196:445–451
Coulam CH, Sheafor DH, Leder RA, Paulson EK, DeLong DM, Nelson RC (2000) Evaluation of pseudoenhancement of renal cysts during contrast-enhanced CT. Am J Roentgenol 174:493–498
Curry NS, Cochran ST, Bissada NK (2000) Cystic renal masses: accurate Bosniak classification requires adequate renal CT. Am J Roentgenol 175:339–342
Dinney CP, Awad SA, Gajewski JB, Belitsky P, Lannon SG, Mack FG, Millard OH (1992) Analysis of imaging modalities, staging systems, and prognostic indicators for renal cell carcinoma. Urology 39:122–129
Foley WD (2003) Renal MDCT. Eur J Radiol 45 (Suppl 1): S73–S78
Fukuya T, Honda H, Nakata H, Egashira K, Watanabe H, Naitou S, Kumazawa J, Masuda K (1994) Computed tomographic findings of invasive transitional cell carcinoma in the kidney. Radiat Med 12:6–10
Hallscheidt PJ, Bock M, Riedasch G, Zuna I, Schoenberg SO, Autschbach F, Soder M, Noeldge G (2004) Diagnostic accuracy of staging renal cell carcinomas using multidetector-row computed tomography and magnetic resonance imaging: a prospective study with histopathologic correlation. J Comput Assist Tomogr 28:333–339
Herr HW (1999) Partial nephrectomy for unilateral renal carcinoma and a normal contralateral kidney: 10-year follow-up. J Urol 161:33–35
Hietala SO, Wahlqvist L (1982) Metastatic tumors to the kidney. A postmortem, radiologic and clinical investigation. Acta Radiol Diagn (Stockh) 23:585–591
Hu H, He HD, Foley WD, Fox SH (2000) Four multidetector-row helical CT: image quality and volume coverage speed. Radiology 215:55–62
Igarashi T, Muakami S, Shichijo Y, Matsuzaki O, Isaka S, Shimazaki J (1994) Clinical and radiological aspects of infiltrating transitional cell carcinoma of the kidney. Urol Int 52:181–184
Jinzaki M, Tanimoto A, Narimatsu Y, Ohkuma K, Kurata T, Shinmoto H, Hiramatsu K, Mukai M, Murai M (1997) Angiomyolipoma: imaging findings in lesions with minimal fat. Radiology 205:497–502
Jinzaki M, Tanimoto A, Mukai M, Ikeda E, Kobayashi S, Yuasa Y, Narimatsu Y, Murai M (2000) Double-phase helical CT of small renal parenchymal neoplasms: correlation with pathologic findings and tumor angiogenesis. J Comput Assist Tomogr 24:835–842
Johnson CD, Dunnick NR, Cohan RH, Illescas FF (1987) Renal adenocarcinoma: CT staging of 100 tumors. Am J Roentgenol 148:59–63
Kallman DA, King BF, Hattery RR, Charboneau JW, Ehman RL, Guthman DA, Blute ML (1992) Renal vein and inferior vena cava tumor thrombus in renal cell carcinoma: CT, US, MRI and venacavography. J Comput Assist Tomogr 16:240–247
Kim JK, Kim TK, Ahn HJ, Kim CS, Kim KR, Cho KS (2002) Differentiation of subtypes of renal cell carcinoma on helical CT scans. Am J Roentgenol 178:1499–1506
Kim JK, Park SY, Shon JH, Cho KS (2004) Angiomyolipoma with minimal fat: differentiation from renal cell carcinoma at biphasic helical CT. Radiology 230:677–684
Kopka L, Fischer U, Zoeller G, Schmidt C, Ringert RH, Grabbe E (1997) Dual-phase helical CT of the kidney: value of the corticomedullary and nephrographic phase for evaluation of renal lesions and preoperative staging of renal cell carcinoma. Am J Roentgenol 169:1573–1578
Leslie JA, Prihoda T, Thompson IM (2003) Serendipitous renal cell carcinoma in the post-CT era: continued evidence in improved outcomes. Urol Oncol 21:39–44
Liu J, Fanning CV (2001) Can renal oncocytomas be distinguished from renal cell carcinoma on fine-needle aspiration specimens? A study of conventional smears in conjunction with ancillary studies. Cancer 93:390–397
Macari M, Bosniak MA (1999) Delayed CT to evaluate renal masses incidentally discovered at contrast-enhanced CT: demonstration of vascularity with deenhancement. Radiology 213:674–680
Neuzillet Y, Lechevallier E, Andre M, Daniel L, Coulange C (2004) Accuracy and clinical role of fine needle percutaneous biopsy with computerized tomography guidance of small (less than 4.0 cm) renal masses. J Urol 171:1802–1805
Novick AC (1992) The role of renal-sparing surgery for renal cell carcinoma. Semin Urol 10:12–15
Pickhardt PJ, Siegel CL, McLarney JK (2001) Collecting duct carcinoma of the kidney: Are imaging findings suggestive of the diagnosis? Am J Roentgenol 176:627–633
Ramani AP, Abreu SC, Desai MM, Steinberg AP, Ng C, Lin CH, Kaouk JH, Gill IS (2003) Laparoscopic upper pole partial nephrectomy with concomitant en bloc adrenalectomy. Urology 62:223–226
Richstone L, Scherr DS, Reuter VR, Snyder ME, Rabbani F, Kattan MW, Russo P (2004) Multifocal renal cortical tumors: frequency, associated clinicopathological features and impact on survival. J Urol 171:615–620
Rubin GD (2001) Techniques for performing multidetector-row computed tomographic angiography. Tech Vasc Interv Radiol 4:2–14
Russo P (2000) Renal cell carcinoma: presentation, staging, and surgical treatment. Semin Oncol 27:160–176
Sagalowsky AI, Kadesky KT, Ewalt DM, Kennedy TJ (1994) Factors influencing adrenal metastasis in renal cell carcinoma. J Urol 151:1181–1184
Sant GR, Heaney JA, Ucci AA Jr, Sarno RC, Meares EM Jr (1984) Computed tomographic findings in renal angiomyolipoma: an histologic correlation. Urology 24:293–296
Sant GR, Ayers DK, Bankoff MS, Mitcheson HD, Ucci AA Jr (1990) Fine needle aspiration biopsy in the diagnosis of renal angiomyolipoma. J Urol 143:999–1001
Sherman JL, Hartman DS, Friedman AC, Madewell JE, Davis CJ, Goldman SM (1981) Angiomyolipoma: computed tomographic–pathologic correlation of 17 cases. Am J Roentgenol 137:1221–1226
Sheth S, Scatarige JC, Horton KM, Corl FM, Fishman EK (2001)

Current concepts in the diagnosis and management of renal cell carcinoma: role of multidetector CT and three-dimensional CT. RadioGraphics 21S237–S254

Smith PA, Marshall FF, Corl FM, Fishman EK (1999) Planning nephron-sparing renal surgery using 3D helical CT angiography. J Comput Assist Tomogr 23:649–654

Staehler G, Brkovic D (2000) The role of radical surgery for renal cell carcinoma with extension into the vena cava. J Urol 163:1671–1675

Studer UE, Scherz S, Scheidegger J, Kraft R, Sonntag R, Ackermann D, Zingg EJ (1990) Enlargement of regional lymph nodes in renal cell carcinoma is often not due to metastases. J Urol 144:243–245

Suggs WD, Smith RB III, Dodson TF, Salam AA, Graham SD Jr (1991) Renal cell carcinoma with inferior vena caval involvement. J Vasc Surg 14:413-418

Sussman S, Cochran ST, Pagani JJ, McArdle C, Wong W, Austin R, Curry N, Kelly KM (1984) Hyperdense renal masses: a CT manifestation of hemorrhagic renal cysts. Radiology 150:207–211

Szolar DH, Kammerhuber F, Altziebler S, Tillich M, Breinl E, Fotter R, Schreyer HH (1997) Multiphasic helical CT of the kidney: increased conspicuity for detection and characterization of small (<3 cm) renal masses. Radiology 202:211–217

Thrasher JB, Paulson DF (1993) Prognostic factors in renal cancer. Urol Clin North Am 20:247–262

Thrasher JB, Robertson JE, Paulson DF (1994) Expanding indications for conservative renal surgery in renal cell carcinoma. Urology 43:160–168

Yuh BI, Cohan RH (1999) Different phases of renal enhancement: role in detecting and characterizing renal masses during helical CT. Am J Roentgenol 173:747–755

Yuh BI, Cohan RH, Francis IR, Korobkin M, Ellis JH (2000) Comparison of nephrographic with excretory phase helical computed tomography for detecting and characterizing renal masses. Can Assoc Radiol J 51:170–176

Zeman RK, Cronan JJ, Rosenfield AT, Lynch JH, Jaffe MH, Clark LR (1988) Renal cell carcinoma: dynamic thin-section CT assessment of vascular invasion and tumor vascularity. Radiology 167:393–396